CIRP Annals - Manufacturing Technology 65 (2016) 233–236

Contents lists available at ScienceDirect

CIRP Annals - Manufacturing Technology

journal homepage: http://ees.elsevier.com/cirp/default.asp

Investigation of hydrodynamic arc breaking mechanism in blasting erosion arc machining

Lin Gu [a], Fawang Zhang [a], Wansheng Zhao [a,*], K.P. Rajurkar (1)[b], A.P. Malshe (1)[c]

[a] State Key Laboratory of Mechanical System and Vibration, School of Mechanical Engineering, Shanghai Jiao Tong University, Shanghai 200240, China
[b] Mechanical and Materials Engineering, University of Nebraska-Lincoln, USA
[c] Mechanical Engineering, University of Arkansas, Fayetteville, AR, USA

ARTICLE INFO

Keywords:
Blasting erosion arc machining (BEAM)
Hydrodynamic arc breaking mechanism (HABM)
Single discharge experiments
Observation research
Spectroscopy
Arc temperature

ABSTRACT

Blasting erosion arc machining (BEAM) greatly improves the material removal rate (MRR) by utilizing the electrical arcs instead of sparks as in EDM. However, the mechanism in BEAM is still not fully understood. By observing and diagnosing the electrical arc generated in a single pulse, the arc temperature is determined and hydrodynamic arc breaking mechanism that can effectively prevent the arcing damage is observed. Furthermore, this paper compares the craters obtained in negative polarity BEAM with that in positive polarity BEAM and explains why the former results in a higher MRR and the latter leads to a better machined surface.

1. Introduction

Machining superalloys, such as nickel-based alloy and titanium alloy, are always a big challenge for the machining industries. Generally, machining these materials with the conventional cutting processes constitutes a large portion of the total part costs because of long cycle time and short cutter life [1]. Therefore, electrical arcing processes are considered for machining these materials with high efficiency. A variant of electro discharge machining process named Arc Dimensional Machining (ADM) was firstly proposed in 1988, which greatly improve the material removal rate (MRR) by utilizing the technological liquid controlled arcs instead of sparks [2]. Electro contact discharge machining or Arc sawing is another arcing process that utilizes an arc to melt and vaporise the workpiece material [3,4]. The process utilizing a rotating steel disk or a linearly travelling metal brand as the electrode is primarily used for fast sectioning of hardened alloys and fragile components. Afterward, the high-speed electro erosion milling [5] and high current density electrical discharge milling [6] took advantage of arcing to mill difficult-to-cut materials resulting in a high MRR. A new high efficiency material removal process named blasting erosion arc machining (BEAM) which is characterized by multi-hole inner flushing was reported in Ref. [7]. By employing a powerful inner flushing controlled arcing, this process is able to remove material in either a milling or die-sinking mode. Furthermore, high efficiency and improved machined surface integrity can be achieved by combining negative and positive polarity BEAM sequentially [8].

Although the BEAM is a stable process with a high machining efficiency, the mechanism of BEAM is still not fully understood. Based on the observation of typical trailing discharge craters, the hydrodynamic arc breaking mechanism was proposed. As shown in Fig. 1, it means that by performing a strong multi-hole inner flushing, the arc plasma column in the discharge gap will be stretched, elongated, or even broken by the strong hydrodynamic force [7]. The preliminary experimental investigations indicate that the HABM (hydrodynamic arc breaking mechanism) can effectively control the arcing and improve the debris expulsion, thereby prevent electric arcing damage on the workpiece surface and stabilize the discharge process [9,10]. Yet this hypothesis still needs to be validated by observation experiments. Although the imported energy in the gap is much larger than that of conventional EDM and results a higher MRR, the thickness of heat effect zone of the BEAMed surface is limited. In order to

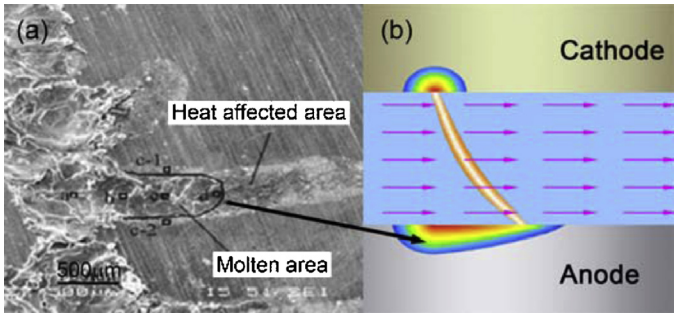

Fig. 1. Trailing discharge craters (a) and hypothesis of hydrodynamic arc breaking mechanism (b).

* Corresponding author. Room 425, Building A, State Key Laboratory of Mechanical System and Vibration, School of Mechanical Engineering, Shanghai Jiao Tong University, 800 Dongchuan Road, Shanghai 200240, China.
Tel.: +86 2134206949.
E-mail address: zws@sjtu.edu.cn (W. Zhao).

http://dx.doi.org/10.1016/j.cirp.2016.04.083
0007-8506/© 2016 CIRP.

comprehensively study the mechanisms in BEAM process, a series of single arc discharge experiments were conducted on a specially designed experimental setup, and the arcing process was observed and diagnosed by using a high-speed video camera and spectrograph. A special debris removal phenomenon was observed and explanation of high MRR as well as thin heat-affected zone (HAZ) is given based on this observation.

2. Experimental setup

The experimental setup consists of observing, flushing and electrical subsystems. Fig. 2 shows the scheme of observing subsystem. Together with a die steel plate electrode, a 2.5 mm diameter copper cylinder electrode with a sharp tip is vertically installed inside the $8 \times 8 \times 150$ mm^3 transparent cubic tube. The gap between the electrodes can be adjusted by a feeding device. The tube with two open sides bridges the inlet and outlet, and enables a controllable powerful flushing. The dielectric flush is supplied by the flushing subsystem which consists of a pump, a dielectric tank and some control valves. In the electrical subsystem, a pulse generator and control switches are used to supply the discharge energy. An oscilloscope with a current sensor and a voltage probe is used to monitor the peak current and inter-electrode voltage during the discharge period. A Phantom V12 high-speed video camera is used to observe and record the discharge process, and the frame frequency is set as 50000 fps in order to capture sufficient details. A research-grade high performance spectrograph, Shamrock 303i, is employed to detect the arcing spectrums. The single discharge experiments were conducted according to the conditions listed in Table 1. After the experiments, the erosion surfaces of the electrodes were analysed by using a Zeiss Stemi 2000-C stereomicroscope.

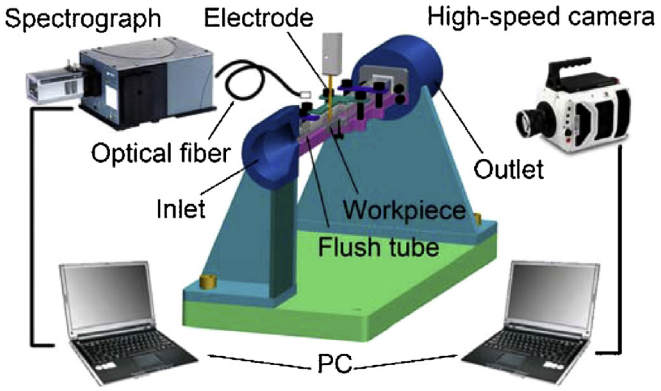

Fig. 2. Scheme of observing subsystem.

Table 1
Single discharge experimental parameters.

Dielectric	Water-based dielectric
Tool material	Copper
Workpiece material	Cr12 die steel
Open voltage u_o, V	90
Peak current i_p, A	50, 100, 200
Pulse duration t_{on}, ms	2, 6, 10
Flush velocity v, m/s	0, 3, 7

3. Results and discussions

3.1. Observation and analysis of HABM

By means of the high-speed camera, the regular process of the arc column shape change caused by the powerful flushing can be clearly observed and obtained, as shown in Fig. 3. The tool electrode's outline was marked on the images as to indicate the

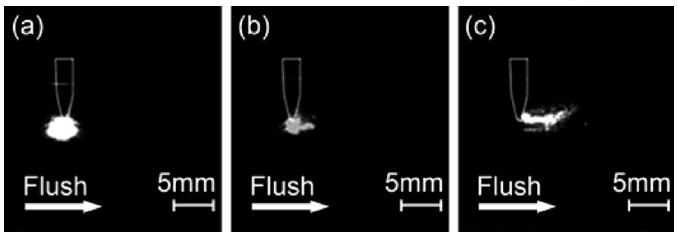

Fig. 3. Comparing of arc column distortion in the flushing dielectric: (a) v = 0 m/s (b) v = 3 m/s (c) v = 7 m/s.

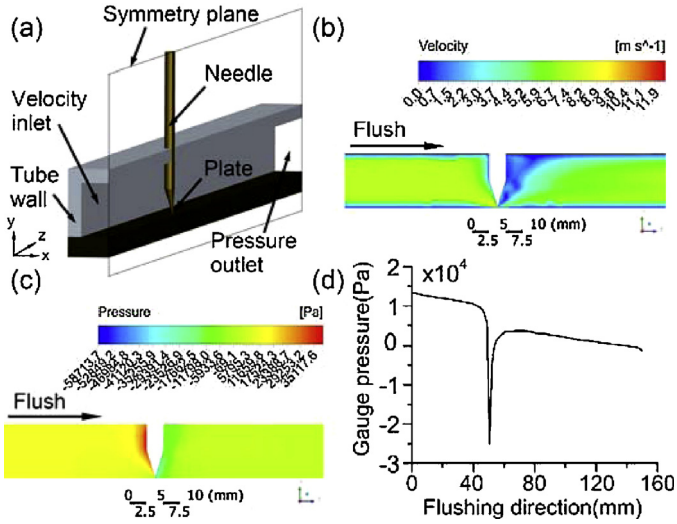

Fig. 4. Simulation of flow field in the tube: (a) Geometric model and boundary conditions (b) Velocity distribution (c) Pressure distribution (d) Pressure distribution along the sampling path.

deformation degree of the arc column. As shown in Fig. 3, the discharge generated a stabilized arc column located in the working gap when the working fluid was motionless. However, with the flushing velocity increasing, the distortion of arc column increased accordingly, and the arc/workpiece interface travelled more than 5 mm along the flushing direction when the flushing velocity was 7 m/s.

In order to study the influence of flushing on the arc column, the flow field in the tube was simulated with the computational fluid dynamics software ANSYS FLUENT 14.5. The boundary conditions are shown in Fig. 4 (a). Inlet velocity was set to 7 m/s according to the measured result, and outlet pressure was set to 0 Pa (gauge pressure). The default wall condition was accepted for all the rest boundaries. In order to work out the pressure variation in the tube, the outlet was taken as the reference pressure location, and the reference pressure was set as 1 atm. According to the Reynolds number calculated from the given conditions, the standard $k-\varepsilon$ viscous model valid for fully turbulent flows was selected. Only 1/2 of the cavity was built in the simulation to reduce the computation burden.

Fig. 4 (b) shows that the dielectric sprays out from the working gap on the downstream side when it flows through the needle electrode at a high velocity. This flow field is favourable to flush away the generated debris from the gap. On the other hand, the contour plot of the pressure distribution indicates that there is a negative pressure zone close to the needle electrode on the downstream side, as shown in Fig. 4 (c). The pressure distribution along the sampling line through the working gap, as shown in Fig. 4 (d), indicates that in the gap the pressure curve falls steeply resulting in a large pressure gradient and a negative pressure zone on the downstream side.

Fig. 5 shows serial images extracted from the discharging video. It can be found that on a cloud the removed debris firstly sprayed out near the working gap on the downstream side at 2.4 ms. After that, the cloud area initially increased with time, and then